IEEE Access
Multidisciplinary ⋮ Rapid Review ⋮ Open Access Journal

Received 5 June 2022, accepted 18 July 2022, date of publication 1 August 2022, date of current version 12 October 2022.

Digital Object Identifier 10.1109/ACCESS.2022.3195279

RESEARCH ARTICLE

Multiview Reconstruction Using Phase Retrieval of Light Field Signals

NAN HE[1], HONG ZHANG[1], AND CHANGJIAN ZHU[2], (Member, IEEE)
[1]Department of Mathematics and Computer Science, Guilin Normal College, Guilin 541001, China
[2]School of Electronic Engineering, Guangxi Normal University, Guilin 541004, China

Corresponding author: Changjian Zhu (changjianzhu@alumni.hust.edu.cn)

This work was supported in part by the China University Industry-University-Research Innovation Fund under Grant 2019ITA01049, in part by the National Natural Science Foundation of China under Grant 61961005, and in part by the Guangxi Natural Science Foundation Project under Grant 2018GXNSFAA281195 and Grant 2019AC20121 (AD19245085).

ABSTRACT Light field rendering is an effective multi-view reconstruction technology. The current multi-view reconstruction methods still have the problem of low view synthesis quality in complex scenes, such as occlusion and non Lambertian surfaces. In this article, we consider a undistorted multiview reconstruction and develop a phase retrieval method for light field (PRLF) signals to improve the rendering quality. Our approach utilizes the phase spectrum in both the time domain and frequency domain of the discrete light field because the phase of the light field carries more scene information. The phase corrections are ''light field truncation'' in the time domain and ''phase replacement'' in the frequency domain. The iterative algorithm used provides high-quality estimated results for the relative phase of the light field. By the estimated phase results, we derive a multiview reconstruction method to improve the rendering quality. Finally, to verify the claimed performance, we also compare the PRLF with the most advanced light field reconstruction algorithms. The experimental results show that the proposed PRLF outperforms other known reconstruction schemes.

INDEX TERMS Light field rendering, phase retrieval, novel view reconstruction, rendering quality.

I. INTRODUCTION

Light field rendering (LFR) [1], [2] is a powerful technique for visualization and human-computer interaction. LFR can ensure good stereo experience and visual immersion by improving the reconstruction quality of a novel view. The reconstruction problem of a novel view given only a set of captured multiview images, as shown in Fig. 1, appears in a wide range of computational imaging and virtual reality applications [3]–[6]. Nonetheless, for the reconstruction of LFR technology [7], the solutions described previously still have some limitations. For instance, reconstruction methods have difficulty generating sufficiently good 3D geometry for foregrounds with complex object shapes or sharp objects with discontinuous depths [8].

Modern novel view quality optimization methods of light fields can be divided into two fundamentally different approaches. The first approach improves the novel view quality by optimizing the capturing of multiview images. By optimizing the capture position and direction of cameras, the most abundant scene information can be obtained to

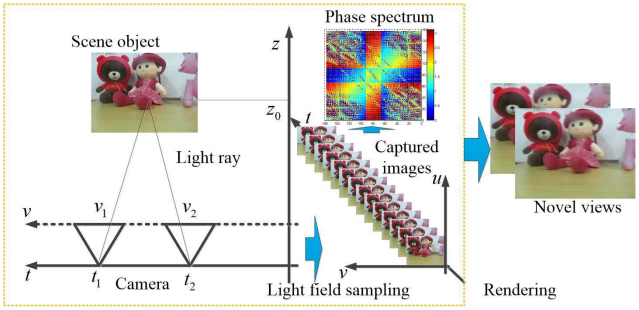

FIGURE 1. Conceptual illustration of the light field. A camera captures scene objects along the camera plane (t, s) in different positions. The captured images can be denoted using image plane (u, v), and then the novel views are rendered by these captured images.

The associate editor coordinating the review of this manuscript and approving it for publication was Eduardo Rosa-Molinar.

improve the rendering quality of novel views, such as active rearranged capturing (ARC) [9], correspondence field (CF) capturing [10], and noncoverage field (NCF) capturing [11]. In this case, the captured position and direction of the camera directly determine the reconstruction quality of novel views. Similar to the capturing of multiview images, the rendering quality of novel views can also be improved by depth information optimization [12], [13]. The second approach improves the quality of novel view reconstruction by optimizing the reconstruction algorithms of the light field. The bandwidth of the light field can be obtained through spectrum analysis, and a reasonable reconstruction filter can be designed to reconstruct the novel views [14]–[17]. Furthermore, learning methods are used to optimize the reconstruction quality of novel views [18]–[21]. In this case, the novel view is used to improve the rendering quality by optimizing the filter bandwidth or learning methods and networks.

The optical detection devices of cameras can only capture the intensity information of light rays but cannot measure the phase information of light rays [22], [23]. Therefore, in the process of light field sampling, the captured image sets contain the light intensity values but lack phase information. The traditional light field reconstruction algorithm only considers the reconstruction and optimization of the amplitude information of the light field. Inspired by the theory of signal phase retrieval [22], [23], along with the development of novel view reconstruction algorithms, this paper considers the fundamental problem of rendering some general novel views. First, we mathematically explore phase retrieval methods for light field (PRLF) signals from a set of captured multiview images. The phase spectral support of a light field signal is bounded by the frequencies along the camera plane and image plane. The phase of the light field is then recovered using a least squares method based on the previous phase retrieval theory of the signal. Second, for the application of PRLF signals to novel view reconstruction from a set of captured multiview images, we try to explore the reconstruction quality optimization method from the phase retrieval direction of the light field signal to improve the rendering quality. Some preliminary results of this paper were presented at a conference [24]. To summarize, our main contributions are as follows:

- Phase recovery is the basis of applied physics and engineering. It is required to determine the phase of a complex-valued function from modulus data and additional a priori information. We apply the theory of phase retrieval to the light field signal and explore the phase retrieval of the light field signal.
- The problem of recovering a signal from the Fourier transform amplitude is of great significance in various fields of engineering, which has existed for more than 100 years. The relationship between novel view reconstruction and phase retrieval of light field signals is derived in detail to improve the viewpoint quality based on phase information.
- The phase of the light field signal contains more scene information. We develop a new novel view reconstruction framework based on light field phase retrieval.

II. RELATED WORK

Since the emergence of light field rendering technology 25 years ago [1], [2], a large number of light field reconstruction technologies have been proposed. We roughly divide these reconstruction technologies into traditional signal processing methods using Fourier transform theory and recent emerging deep learning methods that track and explain the development process of light field reconstruction technology.

A. RECONSTRUCTION USING SPECTRAL ANALYSIS

Traditional research on light field reconstruction using the Fourier transform mainly uses the method of spectrum analysis to estimate the bandwidth of the light field. Then, the novel view rendering quality is designed and optimized according to the light field bandwidth [25]. For example, a linear and spatially invariant reconstruction filter was used in [17], and an appropriate prefilter was used in [16]. Vagharshakyan *et al.* [26] proposed using an adapted discrete shearlet transform to sparse the light field and derived a method of light field reconstruction in the directionally sensitive transform domain. Similar methods and results are also introduced in reference [27]. In [28], Shi *et al.* applied the continuous frequency domain of a light field to sparse light field signals and reconstruct novel views that typically work in the discrete Fourier domain. In [6], a flexible connection scheme of a multilight field system was proposed, and it makes use of the constant radiation of light. Additionally, light field reconstruction by a Fourier disparity layer representation [29] and a concentric multispectral light field [30] can also process the light field through different angles and perform Fourier transforms. Then, the method of light field reconstruction quality optimization is derived by spectrum analysis of the light field for non-Lambertian surface scenes. In [5], Koniaris *et al.* proposed animated light fields with real-time view correlation reconstruction by converting offline rendered movie content into a novel immersive representation. In [31], Marquez *et al.* proposed a compressed spectrum analysis method and a light field imaging architecture based on the principle of a compressed imaging framework to capture the representation of multiplexed multidimensional information. This framework can realize real-time and high-quality view reconstruction.

The above solutions mainly apply the amplitude spectrum of the light field to design the reconstruction filter for novel view reconstruction. However, for complex foreground objects, novel view reconstruction is usually not improved, and more redundant captured images will be generated.

B. RECONSTRUCTION USING LEARNING METHODS

In recent years, with the development of deep learning technology, deep learning has been used to train the captured

multiview images by the light field, and the learning method has been used to study novel multiview reconstruction. For example, in [18] and [32]–[34], Wu *et al.* used a convolutional neural network to train the electronic portal image (EPI) texture structure and then reconstructed the novel views according to the trained EPI texture structure model from a sparse set of captured images. In [20], Farrugia and Guillemot proposed a learning-based superresolution method for deep CNN spatial light fields. The deep CNN spatial light field algorithm allows the restoration of a consistent entire light field in all angular views. In [35], Lamba *et al.* proposed a deep neural network, called L3Fnet, using a two-stage architecture that considers all the light field views to encode the light field geometry and reconstruct each light field view. The proposed L3Fnet can be used to enhance the light field images for low-light light field imaging. In [35], Lamba *et al.* presented a spatio-angular dense network (SADenseNet), which contains two components: correlation blocks and spatio-angular dense skip connections. SADenseNet convolutes the camera plane and the imaging plane using a spatial filter and a angular filter, respectively. There are also a large number of light field-related deep learning methods, such as the multiangular light field angular reconstruction network (MALFRNet) [37], unified learning framework for light field reconstruction [38], Pseudo 4DCNN for depth estimation and view warping of light fields [39], a new learning-based sparse sampled light field with irregular structures [40], and a generation model based on the central view of the light field [41].

The solutions described above mainly use the learning method with the amplitude of the light field to iteratively optimize the reconstruction quality. However, for some complex scenes, such as complex geometry and mutation, and even scenes with occlusion, the reconstructed novel views obtained by deep learning methods are still distorted.

C. PHASE RETRIEVAL FOR SIGNAL

For the captured images of the light field rendering technology, the optical sensor for captured images collects only the amplitude information of the scene, but cannot measure the phase information. Currently, in other areas, there have been many research results on the problem of estimating phase information according to the amplitude information of a signal [42]–[46]. Two detailed surveys of phase retrieval algorithms were described in [22] and [23]. For example, in 1981, Taylor studied in detail the phase recovery problem in the application of electromagnetic theory [47]. In [48], Fienup investigated and compared various solutions to the phase recovery problem. In [49], Klibanov *et al.* investigated various results and explained the only situation in which a signal can be recovered from its amplitude information and supplementary information. In [50], Waldspurger *et al.* solved the phase recovery problem using a provably convergent block coordinate descent algorithm. Candes *et al.* applied matrix completion to study the phase recovery problem [51]. Candes *et al.* also presented a method for phase retrieval using Wirtinger flow in [52]. Sun *et al.* [53] provided a complete geometric characterization of the nonconvex formulation for the generalized phase retrieval problem. This algorithm allows multiple iterations of phase information to find a global minimum without special initialization.

III. LIGHT FIELD SAMPLING MODEL AND FORMULATION

A. LIGHT FIELD REPRESENTATION

We apply 4D light field $p(t, s, v, u)$ [1], [2] quantization to describe the imaging signal of 3D scene, and include camera position and direction, and scene information. (t, s) denotes the camera plane, and (u, v) denotes the image plane. To follow the method of light field representation in [14], [15], and [54]–[57], the 4D light field function $p(t, s, v, u)$ can be simplified to the 2D light field $p(t, v)$ as shown in Fig. 1. The properties and results of the light field signal in the 2D light field (s, u) are the same as those in the 2D light field (t, v). Therefore, we only need to study the results of 2D light field $p(t, v)$. The 2D light field is also named EPI [58], which is the mapping between the scene object and the camera plane and image plane.

B. LIGHT FIELD SAMPLING REQUIREMENTS

For light field sampling, we need to reasonably determine the spacing between two captured cameras. According to the results in [14], [15], and [54]–[57], the spectral support of the light field is with respect to the minimum and maximum depths, the scene texture distribution, the resolution of the sampling camera (Δv), the resolution of the rendering camera, and the scene attribute $\psi(t, v)$. Using the spectral support of the light field, we next define the light field sampling requirements.

Definition 1: Given a scene, the spacing between two captured cameras is determined by the spectral support of the light field [14], [15], [54]–[57]. The spacing between two cameras is calculated as

$$\Delta t_{\max} = \frac{\Delta v \cdot z_{opt} \cdot \psi(t, v)}{f}, \tag{1}$$

where z_{opt} is the optimal depth, and $\psi(t, v)$ affects the light field sampling, such as occlusion, non-Lambertian reflection, texture color change, geometric shapes, and whether the sample is smooth [14], [15], [54]–[57].

Using (1), we can determine the sampling rate of the light field according to specific scene conditions. Special scene conditions include the maximum and minimum depths, object surface geometry and other information. Then, a set of multi-views images for the light field can be captured based on the sampling rate. Using the captured multi-views images, we mathematically derive the light field phase spectrum to reconstruct novel multi-views of the light field in the next section.

C. PROBLEM FORMULATION

According to Fourier series decomposition theory, we can decompose a light field signal into the amplitude and phase.

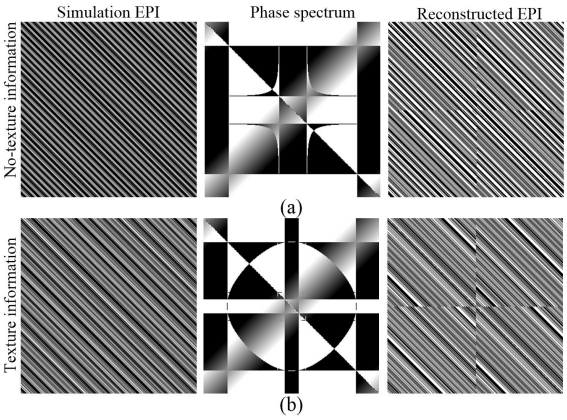

FIGURE 2. Diagram (a) shows an EPI for a sine function of a texture signal; diagram (b) shows the phase light field spectrum.

To analyze the phase of the light field, the 2D light field $p(t, v)$ may be written in terms of its magnitude and phase as

$$p(t, v) = |p(t, v)| \exp\left[j\left(\phi_t(t) + \phi_v(v)\right)\right], \tag{2}$$

where $|p(t, v)|$ denotes the amplitude of the light field, and $\phi_t(t)$ and $\phi_v(v)$ are light field phases for the t-axis and v-axis, respectively.

Generally, the Fourier phase of the light field contains more scene information than the Fourier magnitude [43]. For the captured multi-view image, the optical detection devices of cameras cannot measure the phase of a light wave. The reconstruction of the novel views only uses the amplitude information captured (i.e., $|p(t, v)|$) by the camera. Thus, the phase information is included in the novel view reconstruction, which will improve the reconstruction quality. Therefore, the phase retrieval for light field signals is important. We next define the phase retrieval problem of the light field.

Definition 2: Given a set of captured multi-view images, the phase retrieval problem of the light field can be formulated as

$$\left(\hat{\phi}_t, \hat{\phi}_v\right) = \underset{(\phi_t, \phi_v)}{\arg\min} \left(\left| |p(t, v)| \cdot \exp\left(\hat{\phi}_t + \hat{\phi}_v\right) - p(t, v) \right|^2 \right). \tag{3}$$

where $\left(\hat{\phi}_t, \hat{\phi}_v\right)$ are the phase retrieval of light field.

We mathematically explore the phase retrieval method of light field signals for application to novel view reconstruction. The phase spectral support of a light field signal is bounded by the frequencies along the camera plane and image plane. The phase of the light field is then recovered using a least squares method based on the previous phase retrieval theory of the signal.

IV. PHASE SPECTRUM ANALYSIS OF THE LIGHT FIELD

A. LIGHT FIELD PHASE SPECTRUM

To analyze the phase characteristics of the light field, we sample the continuous light field by (n_t, m_v) to obtain the discrete light field, denoted by $p(n_t, m_v)$. The z-transform of $p(n_t, m_v)$, denoted by $P(z_t, z_v)$, is defined by

$$P(z_t, z_v) = \sum_{n_t} \sum_{m_v} p(n_t, m_v) z^{-n_t} z^{-m_v}. \tag{4}$$

The Fourier transform is the z-transform on the unit circle. Thus, the Fourier transform of the discrete light field exists and is given by

$$\begin{aligned} P(\omega_t, \omega_v) &= P(z_t, z_v)|_{z_t = \exp(j\omega_t), z_v = \exp(j\omega_v)} \\ &= \sum_{n_t} \sum_{m_v} p(n_t, m_v) \exp\left(-j\left(n_t\omega_t + m_v\omega_v\right)\right). \end{aligned} \tag{5}$$

The Fourier transform result of the light field can also be regarded as a function of the amplitude and phase

$$P(\omega_t, \omega_v) = |P(\omega_t, \omega_v)| \exp\left[j\left(\Phi_t(\omega_t) + \Phi_v(\omega_v)\right)\right], \tag{6}$$

where $\Phi_t(\omega_t)$, and $\Phi_v(\omega_v)$ are the Fourier transforms of $\phi_t(t)$ and $\phi_v(v)$, respectively. Based on (2) and (6), we now state the light field phase spectrum in the following theorem.

Theorem 1: The light field phase is calculated by

$$\begin{aligned} \hat{\Phi}_t(\omega_t) &= \arctan\left(\frac{P_I(\omega_t, \cdot)}{P_R(\omega_t, \cdot)}\right), \hat{\Phi}_v(\omega_v) \\ &= \arctan\left(\frac{P_I(\cdot, \omega_v)}{P_R(\cdot, \omega_v)}\right). \end{aligned} \tag{7}$$

The light field phase spectrum is calculated by

$$\hat{\phi}(\omega_t, \omega_v) = arc\tan\left(\frac{P_I(\omega_t, \omega_v)}{P_R(\omega_t, \omega_v)}\right). \tag{8}$$

where $P_R(\omega_t, \omega_v)$ is the real part of $P(\omega_t, \omega_v)$, and $P_I(\omega_t, \omega_v)$ is the imaginary part of $P(\omega_t, \omega_v)$.

Proof: See Appendix A.

By (8), we can calculate the phase spectrum of the light field. We use a sine function to construct a light field with the texture information as shown in Fig. 2(a), and the corresponding phase spectrum of the light field is presented in Fig. 2(b). The phase spectrum consists of six parallel oblique lines. These six parallel phase spectra are important information for constructing the light field.

B. LIGHT FIELD PHASE OPTIMIZATION

As noted before, the optical phase of the light field signal cannot be directly measured by an electronic detector. The electronic detector of the camera only measures the magnitude of the light field. By (7) and (8), the phase spectrum of the light field can be derived from the frequency along camera axis ω_t and image axis ω_v. However, we are not able to obtain the mathematical relationship between the phase and amplitude from (7) and (8) because the camera can only measure the amplitude of the light field for the captured multi-view images. Based on the results in [54]–[57], the spatial frequency ω_t and imaging frequency ω_v of light field can be derived using the captured multi-view images. Thus, we optimize the phase spectrum estimation of the

light field in (7) and (8) using the captured multi-view images.

In light field sampling, we often have access only to the Fourier magnitudes of a light field signal $p(t, v)$, i.e., $|P(\omega_t, \omega_v)|$. The phase information of the light field is hard or infeasible to record due to physical constraints. The problem of optimizing the light field signal $p(t, v)$ from its Fourier magnitudes $|P(\omega_t, \omega_v)|$ is naturally termed (Fourier) phase optimization. Given N captured multi-view images, the captured multi-view images are described by the 2D light field $|p_k(t, v)|, k = 1, \cdots, N$ (Only including the amplitude information) and multi-view image acquisition vector $p_1(n_t, m_v), \cdots, p_n(n_t, m_v) \in C^n$. In discrete 2D Fourier phase retrieval of the light field, the measurement vectors of the light field correspond to $p_k(n_t, m_v) = e^{-j2\pi(k(n_t, m_v))/N}$.

The optimized phase spectrum estimation of the light field can be considered a distortion free novel view reconstruction from the captured multi-view images. According to Fourier theory, the distortion free novel view reconstruction of the light field $p(t, v)$ from the measurement of $P(\omega_t, \omega_v)$ can be achieved by simply applying the inverse-DFT operator, i.e., $P(\omega_t, \omega_v) = |P(\omega_t, \omega_v)| . e^{j\hat{\phi}(\omega_t, \omega_v)}$. The Fourier phase-optimized problem is to optimize $p(t, v)$ when only the magnitude of $P(\omega_t, \omega_v)$ is measured, i.e., to optimize $p(n_t, m_v)$ given $|P(\omega_t, \omega_v)|$. Since the DFT operator is bijective, this is equivalent to optimizing the phase of $P(\omega_t, \omega_v)$, i.e., $\phi(\omega_t, \omega_v)$-hence the term phase is optimized. We next define the phase optimization of light field.

Definition 3: Generalized phase optimized problem of the light field: Is it possible to efficiently recover an unknown light field $p(t, v)$ from Fourier magnitudes $|P(\omega_t, \omega_v)|$ of discrete light field signal $p_k(n_t, m_v), k = 1, \cdots, N$, up to a global phase factor $e^{j\phi(\omega_t, \omega_v)}$?

The Fourier magnitudes $|P(\omega_t, \omega_v)|$ of light field projections onto a set of captured multi-view images, i.e., $p_1(n_t, m_v), \cdots, p_n(n_t, m_v) \in C^n$. The Fourier magnitudes can be written as

$$|P(\omega_t, \omega_v)| = |\langle p_k(n_t, m_v), p(t, v)\rangle| \, (k = 1, \cdots, N). \quad (9)$$

Obviously, we hope to recover $p(t, v)$ up to a global phase, as $p(t, v) = |p(t, v)| e^{j\phi(\omega_t, \omega_v)}$ for all $\phi(\omega_t, \omega_v) \in [0, 2\pi)$ provides exactly the same set of captured multi-view images. The Fourier phase-optimization problem is as a special case of the more general phase-optimization problem, where we are given a set of captured multi-view images.

As opposed to these strategies, we solve the phase optimization problem by explicitly separating the amplitude and phase variables, and by only optimizing the values of the phase variables. Given a set of captured multi-view images, the phase optimization problem of the light field can thus be written as

$$\min_{p(t,v)} \sum_{k=1}^{N} \| \langle p_k(n_t, m_v), p(t, v)\rangle - diag(|P_k(\omega_t, \omega_v)|) \phi_k(\omega_t, \omega_v) \|_2^2 . \quad (10)$$

where $diag(\cdot)$ denotes a diagonal matrix. We optimize both variables $\phi_k(\omega_t, \omega_v) \in C^n$ and $p(t, v) \in C^p$.

Specifically, we define an $N \times N$ matrix $P = P_i(\omega_t, \omega_v) \cdot P_j^*(\omega_t, \omega_v), i, j = 1, 2, \cdots, N$. Based on (10), we now state the phase optimized on a novel view of the light field in the following theorem.

Theorem 2: For a light field signal, given N captured multi-view images $p_k(n_t, m_v)$, the phase of the light field can be balanced and optimized using the amplitude spectrum of the light field as

$$\hat{\phi}(\omega_t, \omega_v) \approx \frac{1}{N} \sum_{i=1}^{N} \frac{-\sum_{j \neq i} M_{ij} arc\tan\left(\frac{P_I(\omega_t, \omega_v)}{P_R(\omega_t, \omega_v)}\right)}{\left|\sum_{j \neq i} M_{ij} arc\tan\left(\frac{P_I(\omega_t, \omega_v)}{P_R(\omega_t, \omega_v)}\right)\right|}, \quad (11)$$

where the Hermitian matrix $M_{i,j} = diag\left(P_{i,j}\right)\left(I - A_{i,j}\right)$ $diag\left(P_{i,j}\right)$ is positive semidefinite, and $A = p_k(n_t, m_v) \cdot p_k^*(n_t, m_v), k = 1, 2, \cdots, N$. For each $i = 1, \cdots, N$, when $\phi(\omega_t, \omega_v)$ is the optimum solution to the phase recovery problem of the light field signal, $\hat{\phi}(\omega_t, \omega_v)$ amounts to solving

$$\min_{\left|\hat{\phi}(\omega_t, \omega_v)\right|=1} Re\left(\hat{\phi}(\omega_t, \omega_v) \sum_{j \neq i} M_{i,j} \hat{\phi}^*(\omega_t, \omega_v)\right), \quad i = 1, 2, \cdots, N. \quad (12)$$

Proof: The full proof can be found in Appendix B.

Using Theorem 2, we can estimate and optimize the phase spectrum of the light field by using the amplitude information of the captured multi-view images. The optimized phase spectrum carries more abundant scene information.

V. RECONSTRUCTION MODEL OF NOVEL VIEWS

A. RECONSTRUCTION MODEL

Based on the above phase spectrum of the light field, we derive a reconstruction model. It is always possible to find another discrete light field that has a Fourier transform with the same phase by simply convolving $p(n_t, m_v)$ with a zero phase sequence $g(n_t, m_v)$; i.e.,

$$\hat{p}(n_t, m_v) = p(n_t, m_v) * g(n_t, m_v), \quad (13)$$

where $*$ denotes the convolution operation. In the frequency domain, the form for multiplying two functions is

$$\begin{aligned} \hat{P}(\omega_t, \omega_v) &= P(\omega_t, \omega_v)\left[\hat{P}(\omega_t, \omega_v) \Big/ P(\omega_t, \omega_v)\right] \\ &= P(\omega_t, \omega_v) \cdot G(\omega_t, \omega_v). \end{aligned} \quad (14)$$

Thus,

$$\hat{\phi}(\omega_t) = \phi_p(\omega_t) + \phi_g(\omega_t), \hat{\phi}(\omega_v) = \phi_p(\omega_v) + \phi_g(\omega_v). \quad (15)$$

If $\hat{\phi}(\omega_t) = \phi_p(\omega_t)$, then $\phi_g(\omega_t) = 0$. If $\hat{\phi}(\omega_v) = \phi_p(\omega_v)$, then $\phi_g(\omega_v) = 0$. For the zero phase function, the estimation of the phase function is

$$n_0 = \frac{1}{\pi}\left[\hat{\phi}_t(\pi) - \hat{\phi}_t(0)\right], n_1 = \frac{1}{\pi}\left[\hat{\phi}_v(\pi) - \hat{\phi}_v(0)\right]. \quad (16)$$

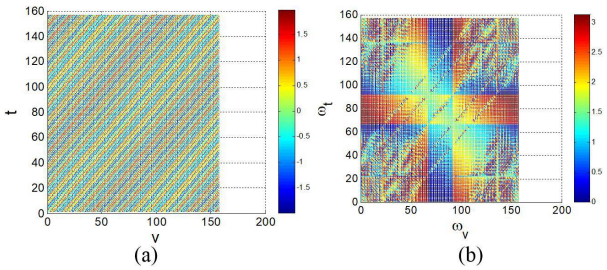

FIGURE 3. Reconstruction of the simulated EPI using the PSAM method relies on the phase spectrum. (a) The simulated EPI and its reconstruction EPI without considering the texture information; (b) the results with respect to a texture signal.

$$\phi(\omega_t) = \hat{\phi}_t(\omega_t) - n_0\omega_t - \hat{\phi}_t(0). \quad (17)$$

$$\phi(\omega_v) = \hat{\phi}_v(\omega_v) - n_0\omega_v - \hat{\phi}_v(0). \quad (18)$$

The PRLF is presented for reconstructing a discrete light field from samples of the phase of its Fourier transform. Therefore, a heuristic approach for reconstructing $\hat{p}(n_t, m_v)$ is an iterative algorithm. This algorithm is characterized by the repeated transformation between the time and frequency domains where, in each domain, the known information about the desired sequence is imposed on the current estimate light field.

B. RECONSTRUCTION METHOD BY A PHASE OF THE LIGHT FIELD

Based on the above phase spectrum analysis and Theorem 1, we derive the light field reconstruction method using the phase information. For the reconstruction method of the light field, given a discrete light field $p(n_t, m_v)$, whose Fourier transform is expressed as $P(\omega_t, \omega_v)$, the light field reconstructed with the above estimated phase is expressed as

$$\begin{aligned}\hat{P}(\omega_t, \omega_v) &= |P(\omega_t, \omega_v)| \exp\left(j\hat{\phi}(\omega_t, \omega_v)\right) = |P(\omega_t, \omega_v)| \\ &\cdot \exp\left(j\frac{1}{N}\sum_{i=1}^{N}\frac{-\sum_{j\neq i} M_{ij} arc\tan\left(\frac{P_I(\omega_t,\omega_v)}{P_R(\omega_t,\omega_v)}\right)}{\left|\sum_{j\neq i} M_{ij} arc\tan\left(\frac{P_I(\omega_t,\omega_v)}{P_R(\omega_t,\omega_v)}\right)\right|}\right). \quad (19)\end{aligned}$$

The reconstructed light field can be obtained by the inverse Fourier transform of (19) as follows:

$$\begin{aligned}\hat{p}(n_t, m_v) &= IDFT\left[\hat{P}(\omega_t, \omega_v)\right] \\ &= IDFT\left[|P(\omega_t, \omega_v)| \exp\left(j\hat{\phi}(\omega_t, \omega_v)\right)\right]. \quad (20)\end{aligned}$$

Based on (19) and (20), we simulate two EPI signals as shown in Fig. 3. One EPI signal is simulated without complex texture information. The other EPI signal contains complex texture information. Then, the PRLF is used to reconstruct the EPI, and the results are shown in Fig. 3. From the results, we find that the two EPIs cannot be well reconstructed. The reason is that the phase estimation of the EPI is inaccurate. Thus, the phase estimation of the light field needs to be further optimized for novel view reconstruction.

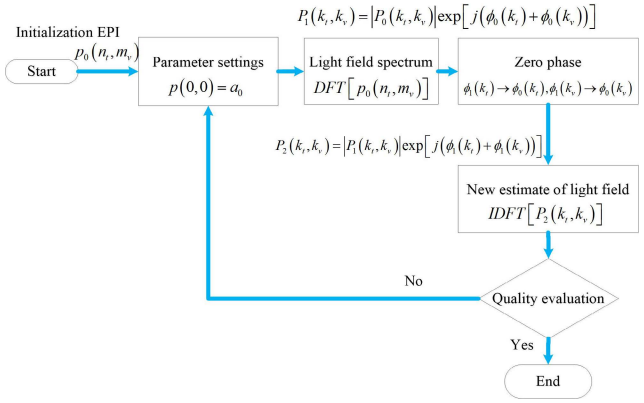

FIGURE 4. Flow chart of light field phase retrieval algorithm for static scenes.

C. ITERATIVE RECONSTRUCTION ALGORITHM

To optimize the quality of novel view reconstruction, we can optimize the reconstruction method in (20) based on time-frequency conversion theory [42]. Based on (19) and (20), we develop an iterative algorithm to optimize the quality of novel view reconstruction, which can start from the phase spectrum reconstruction of the captured multi-view images that meet certain conditions. Each iteration of the algorithm includes two transformations from the spatial domain to the frequency domain and from the frequency domain to the spatial domain of the light field signal, and includes two modifications in the time domain and the frequency domain of the light field signal. Thus, the quality of the reconstructed novel views is improved with each iteration.

The PRLF is presented for reconstructing a discrete light field from samples of the phase of its Fourier transform. Therefore, a heuristic approach for reconstructing $p(n_t, m_v)$ is an iterative algorithm. This algorithm is characterized by the repeated transformation between the time and frequency domains where, in each domain, the known information about the desired sequence is imposed on the current estimate light field. Additionally, the iteration may be described as follows.

Input: $|p(n_t, m_v)|$, $|P(\omega_t, \omega_v)|$, $\in$.

$|p(n_t, m_v)|$-Real-space magnitude.

$|P(\omega_t, \omega_v)|$-Fourier magnitude.

$\in$-Error threshold.

Output: $p_{out}(n_t, m_v)$- a vector that conforms with both magnitude constraints, i.e., : $|p_{out}(n_t, m_v)| = |p(n_t, m_v)|$, and $|P_{out}(\omega_t, \omega_v)| = |P(\omega_t, \omega_v)|$, where $P_{out}(\omega_t, \omega_v)$ is the DFT of $p_{out}(n_t, m_v)$.

Initialization: Choose initial $p_0(n_t, m_v) = |p(n_t, m_v)| \exp(\phi(\omega_t, \omega_v))$ (e.g., with a random phase $\phi(\omega_t, \omega_v)$).

•*Step 1:* Beginning with the spectrum of the initial light field $p_0(n_t, m_v)$, i.e., $P_0(\omega_t, \omega_v) = DFT[p_0(n_t, m_v)]$, an initial guess of the unknown DFT magnitude, the first estimated light field $P_1(\omega_t, \omega_v)$ of the initial light field spectrum $P_0(\omega_t, \omega_v)$ is formed by combining $P_0(\omega_t, \omega_v)$ with the

random phase $\phi(\omega_t, \omega_v)$, i.e.,

$$P_1(\omega_t, \omega_v) = |P_0(\omega_t, \omega_v)| \exp[j\phi(\omega_t, \omega_v)]. \quad (21)$$

Computing the inverse DFT of $P_1(\omega_n, \omega_m)$ provides the first estimate light field, $p_1(n_t, m_v)$, of $p_0(n_t, m_v)$. Because the light field signal has zero phase in the frequency domain, $p_1(n_t, m_v)$ is equal to $p_0(n_t, m_v)$ within a scale factor.

•*Step 2:* From $p_0(n_t, m_v)$, another discrete light field, $p_1(n_t, m_v)$, is formed as follows:

$$p_1(n_t, m_v) = \begin{cases} p_0(n_t, m_v), & for\ n_t < N, m_v < M and n \neq 0 \\ A, & for, n = 0 \\ 0, & otherwise \end{cases} \quad (22)$$

•*Step 3:* The magnitude $P_1(\omega_t, \omega_v)$ of the DFT of $p_1(n_t, m_v)$ is then used as the new estimated light field of $P_2(\omega_t, \omega_v)$ and the next estimated light field of $P_2(\omega_t, \omega_v)$ is formed by

$$P_2(\omega_t, \omega_v) = |P_1(\omega_t, \omega_v)| \exp[j\phi(\omega_t, \omega_v)]. \quad (23)$$

A new estimated light field, $p_2(n_t, m_v)$, is then obtained by taking the inverse DFT of $P_2(\omega_t, \omega_v)$. The repeated application of steps two and three defines the iteration.

$$p_2(n_t, m_v) = IDFT[P_2(\omega_t, \omega_v)]. \quad (24)$$

Until: $E = \sum_k ||P_2(\omega_t, \omega_v) - P_{out}(\omega_t, \omega_v)||^2 \leq \in$.

The flowchart of the above light field reconstruction steps is also shown in Fig. 4.

VI. EXPERIMENTAL RESULTS AND ANALYSIS

A. LIGHT FIELD PHASE SPECTRUM ANALYSIS

We tested our light field phase spectrum algorithm on two real datasets: ragdoll and orchid, where the scenes are shown in the top of Fig. 5. Each scene includes 200 images uniformly captured at different positions, with each image having a pixel values of 320*240. Then, the 200 captured images compose EPI, and a 2D Fourier transform is performed on the EPI to obtain the phase spectrum presented in Figs. 5(a) and (b). It can be found that the series of parallel phase lines are not visible in the ω_t, ω_v-plane. The reason for this phenomenon is the complexity of the scene, which makes the light field signal not just a periodic signal. There are other noise and interference signals that make the phase parallel lines inconspicuous. The more complicated the scene, the more cluttered the phase spectrum, this effect is shown by the differences in Figs. 5(a) and (b). Therefore, we can use the phase spectrum to iteratively modify the phase of the light field to obtain the light field information and improve the rendering quality.

B. COMPARISON OF LIGHT FIELD RECONSTRUCTION

To evaluate the performance of the PRLF in improving the quality of LFR, we use synthetic scenes and actual scenes to reconstruct the light field. Each scene captures a set of images

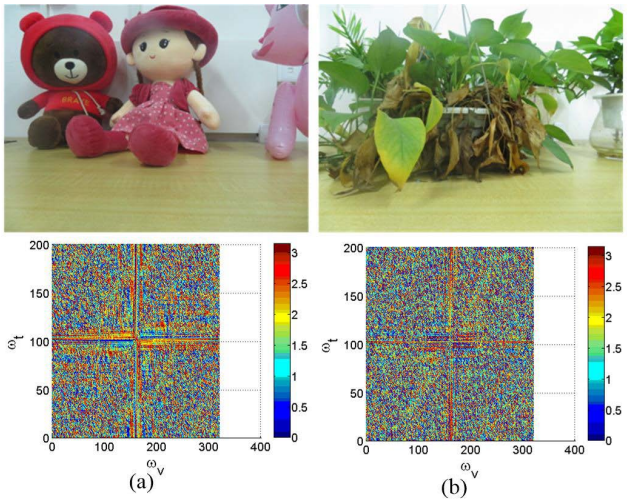

FIGURE 5. Phase spectrum of the light field for two actual scenes: ragdoll and orchid. (a) The ragdoll scene and its phase spectrum; (b) the orchid scene and its phase spectrum.

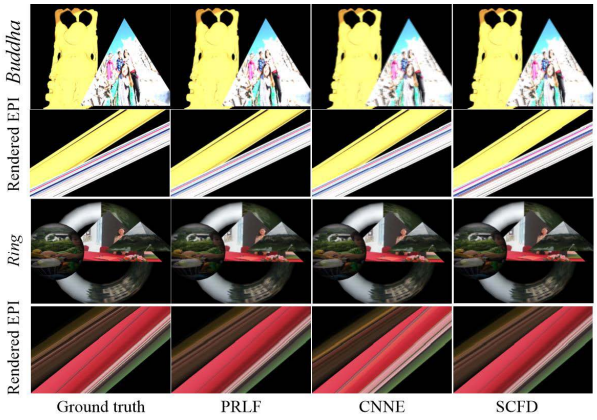

FIGURE 6. Rendered novel views and the corresponding rendered EPIs for two synthetic scenes.

(the sampling rate is calculated by [14]) uniformly at different positions, and then these captured images are used for rendering novel views. Additionally, 200 novel multiviews are reconstructed for each scene. The reconstruction method considers three models: the PRLF, light field reconstruction model using a convolutional network on the EPI (CNNE) by Wu *et al.* [18] and light field reconstruction using sparsity in the continuous Fourier domain (SCFD) by Shi *et al.* [28].

1) SYNTHETIC SCENES

To verify that our PRLF can improve the rendering quality of the light field, we capture images from datasets and reconstruct views using two synthetic scenes (buddha [59] and ring by 3ds Max) depicted in Fig. 6. The light field reconstruction results in Fig. 6 show that the novel views reconstructed using the PRLF, SCFD and CNNE methods have similar effects. The reconstruction results have no obvious distortion. For example, for the Buddha scene, the reconstructed results

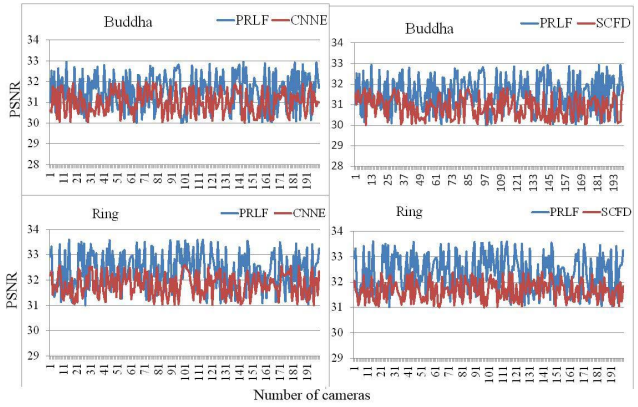

FIGURE 7. PSNRs of 200 rendered novel views for different methods and synthetic scenes.

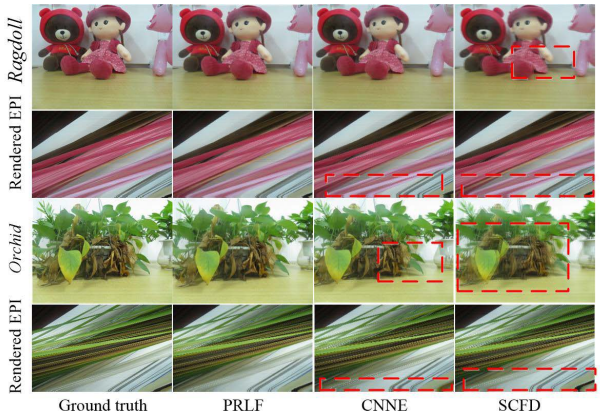

FIGURE 8. Rendered novel views and corresponding rendered EPIs for two actual scenes.

do not show distortion. A similar phenomenon can be seen from either the reconstructed EPI or a single rendered view. The quality of the rendered views is measured by the peak signal-to-noise ratios (PSNRs) against the ground truth image as shown in Fig. 7. Furthermore, similar phenomena can be seen from the reconstructed EPI and novel views of the ring scene. From these experimental results, we find that the PRLF has good light field reconstruction.

2) INDOOR ACTUAL SCENES

We evaluate the proposed approach using two ragdoll and orchid indoor scenes, as depicted in Fig. 5. For the rendering results, we find that the quality of the reconstructed novel views using these three methods is better and the distortion is less. Only a few reconstructed viewpoints still have distortions. Fig. 8 shows that the reconstructed views have some obvious ghosting and aliasing in either the ragdoll scene or the orchid scene. Apparently, the rendering quality of the PRLF is better than that of the CNNE and SCFD on the ragdoll scene. Ghosting occurs because scene complexities, such as leafage and irregular shape, are challenging to reconstruct accurately. However, when using the PRLF, ghosting and aliasing in the rendered views decrease. There are identical phenomena that occur in the orchid scene. These results also suggest that the PRLF can be applied to analyze complex scenes for light field reconstruction.

3) OUTDOOR ACTUAL SCENES

To evaluate the performance of our method, 30 novel views of two actual outdoor scenes are reconstructed using the collected data according to the following methods: the PRLF, CNNE and SCFD. The rendering results are shown in Fig. 9. We find that the quality of the reconstructed novel views using these three methods is better and the distortion is less. This novel view reconstruction comparison experiment, also shows that PRLF has good novel view reconstruction performance. The main reason is that PRLF uses scene phase information, which improves the quality of the rendered views.

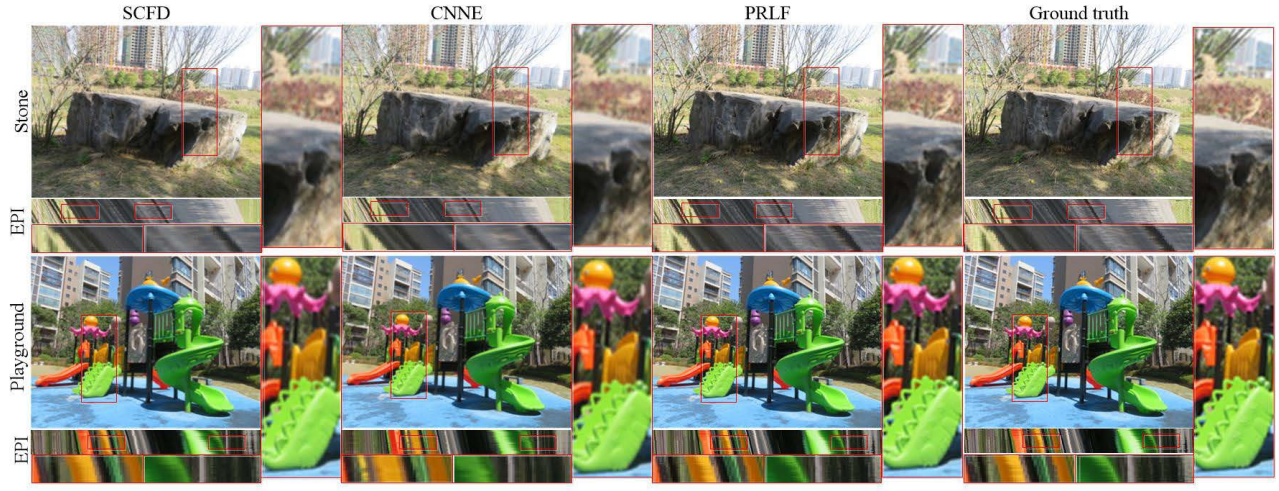

FIGURE 9. Using the PRLF, CNNE, and SCFD to render novel views and the corresponding rendered EPIs for actual outdoor scenes, i.e., Stone, and Playground.

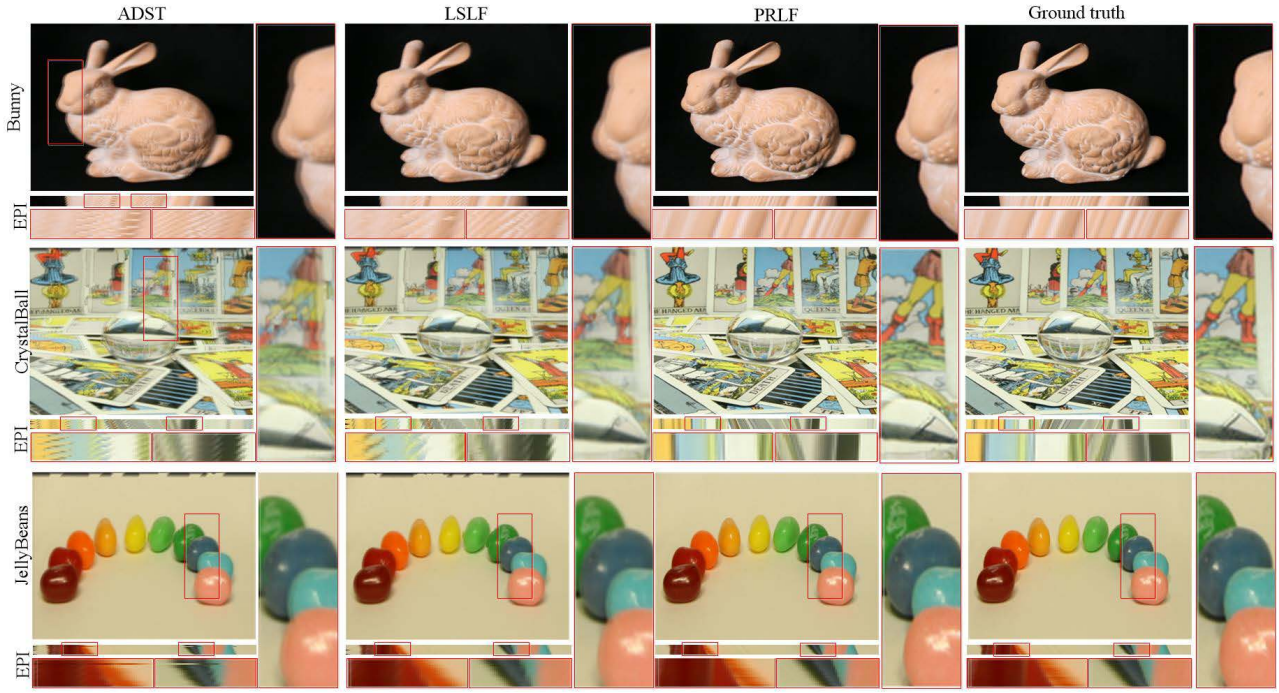

FIGURE 10. Using the PRLF, LSLF, and ADST to render novel views and the corresponding rendered EPIs on the three published datasets of the Stanford light field archive, i.e., Bunny, Crystal Ball, and Jelly Beans [59].

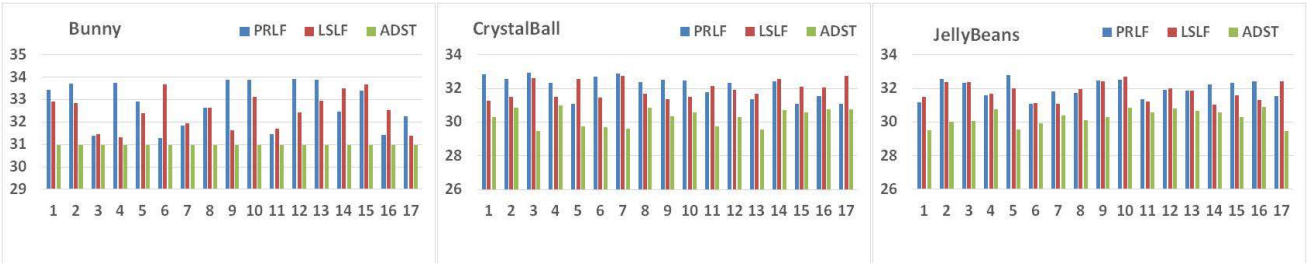

FIGURE 11. PSNRs obtained by the three methods, PRLF, LSLF, and ADST, on the three scenes, Bunny, Crystal Ball, and Jelly Beans.

C. COMPARISON ON PUBLICLY AVAILABLE DATASETS

To further compare and evaluate the performance of the PRLF method with that of other methods, we select three published datasets form the Stanford light field archive, i.e., Bunny, Crystal Ball, and Jelly Beans [59], for comparison experiments. Seventeen novel views are reconstructed by the PRLF, learning-based spatial light field (LSLF) super-resolution method [20], and adapted discrete shearlet transform (ADST) [26].

The rendering results for the EPIs of the three scenes using the three different methods are presented in Fig. 10. From the Bunny scene, the rendered views by the three methods do not experience distortion. However, the rendered EPI using the ADST method has some distortion. When the PRLF and LSLF methods are used, the reconstructed EPIs have no distortion and have better reconstruction quality. For the Crystal Ball scene, the views rendered by the three methods do not experience distortion, and there are good reconstruction effects. However, the rendered EPIs with ADST and LSLF have a small amount of distortion and blur. Similar phenomena can also be seen in the Jelly Beans scene. Therefore, the views rendered by the PRLF method have better display results. These results also have the same change trend as the PNSR statistical results in Fig. Fig. 11. The excellent performance of the PRLF reconstruction method is due to the use of optimized light field phase information, which depends on the large amount of scene information contained in the phase spectrum.

VII. CONCLUSION

In this paper, we proposed a PRLF model for LFR using phase spectrum theory. This reconstruction model has been studied, and its spectrum is presented. We present a light field reconstruction algorithm based on phase iterative correction. Based on the phase spectrum correction, novel views of the

light field can be reconstructed. Furthermore, the rendering quality of the light field can be improved for complex scenes.

For the multi-view synthesis of light field technology, the quality of rendered novel views will decline for complex scenes. We increase the captured information of scene from the phase recovery of light field signal, so as to improve the rendering quality. Based on the traditional signal phase recovery works, our work provides a study method of LFR technology. However, there are still some shortcomings in our work on the method of light field phase recovery. The main reason is that light field phase recovery is related to scene information. In our our future work, we will study phase recovery of light field associated with scene information.

VIII. PROOF OF THEOREM 1

Proof: Since $P(\omega_t, \omega_v)$ is, in general, a complex-valued function of the light field, it may be expressed in terms of its real and imaginary parts as follows:

$$P(\omega_t, \omega_v) = P_R(\omega_t, \omega_v) + j \cdot P_I(\omega_t, \omega_v), \tag{25}$$

where

$$|P(\omega_t, \omega_v)|^2 = [P_R(\omega_t, \omega_v)]^2 + [P_I(\omega_t, \omega_v)]^2, \tag{26}$$

and

$$\tan[\Phi_t(\omega_t)] = \frac{P_I(\omega_t, \cdot)}{P_R(\omega_t, \cdot)}, \tan[\Phi_v(\omega_v)] = \frac{P_I(\cdot, \omega_v)}{P_R(\cdot, \omega_v)}. \tag{27}$$

By (27), we can calculate the phase spectrum of the light field. We use a sine function to construct a light field with the texture information as shown in Fig. 2(a), and the corresponding phase spectrum of the light field is presented in Fig. 2(b). The phase spectrum consists of six parallel oblique lines. These six parallel phase spectra are important information for constructing the light field.

$$\begin{aligned} \hat{\Phi}_t(\omega_t) &= \arctan\left(\frac{P_I(\omega_t, \cdot)}{P_R(\omega_t, \cdot)}\right), \\ \hat{\Phi}_v(\omega_v) &= \arctan\left(\frac{P_I(\cdot, \omega_v)}{P_R(\cdot, \omega_v)}\right). \end{aligned} \tag{28}$$

$$\hat{\phi}(\omega_t, \omega_v) = arc\tan\left(\frac{P_I(\omega_t, \omega_v)}{P_R(\omega_t, \omega_v)}\right). \tag{29}$$

IX. PROOF OF THEOREM 2

Proof: By (10), the inner minimization problem in $p(t, v)$ is a standard least squares and can be solved explicitly by setting

$$p(t, v) = \sum_{k=1}^{N} A \cdot diag(|P_k(\omega_t, \omega_v)|)\, \phi_k(\omega_t, \omega_v), \tag{30}$$

where $A = p_k(n_t, m_v) \cdot p_k^*(n_t, m_v), k = 1, 2, \cdots, N$. In (30), light field view reconstruction is equivalent to the reduced problem

$$\min_{\substack{\left|\hat{\phi}(\omega_t,\omega_v)\right|=1, \\ \hat{\phi}(\omega_t,\omega_v)\in C^n}} \left\| Adiag(P)\,\hat{\phi}(\omega_t, \omega_v) - diag(P)\,\hat{\phi}(\omega_t, \omega_v) \right\|_2^2. \tag{31}$$

The objective of this last problem can be rewritten as follows

$$\begin{aligned} &\left\| Adiag(P) - diag(P)\,\hat{\phi}(\omega_t, \omega_v) \right\|_2^2 \\ &= \left\| (A - I)\, diag(P)\,\hat{\phi}(\omega_t, \omega_v) \right\|_2^2 \\ &= \hat{\phi}^*(\omega_t, \omega_v)\, diag\left(P^T\right) \tilde{M}\, diag(P)\,\hat{\phi}(\omega_t, \omega_v), \end{aligned} \tag{32}$$

where $\tilde{M} = (A - I)^* (A - I) = I - A$. Finally, the phase recovery problem (30) becomes

$$\begin{aligned} &\min\left(\hat{\phi}^*(\omega_t, \omega_v)\, M \hat{\phi}(\omega_t, \omega_v)\right), \\ &subject\ to \left|\hat{\phi}(\omega_t, \omega_v)\right| = 1. \end{aligned} \tag{33}$$

where the Hermitian matrix $M = diag(P)(I - A)\, diag(P)$ is positive semidefinite.

Having transformed the phase recovery problem (30) in the quadratic minimization problem (31), suppose that we are given an initial vector $diag(P)\,\hat{\phi}(\omega_t, \omega_v)$, and focus on optimizing over a single component $\hat{\phi}(\omega_t, \omega_v)$. The problem is equivalent to solving

$$\begin{aligned} \min &\left(\begin{array}{l} \hat{\phi}^*(\omega_t, \omega_v)\, M \hat{\phi}(\omega_t, \omega_v) \\ +2Re\left(\sum_{j\neq i} \hat{\phi}(\omega_t, \omega_v)\, M_{i,j} \hat{\phi}^*(\omega_t, \omega_v)\right) \end{array}\right), \\ &\left|\hat{\phi}(\omega_t, \omega_v)\right| = 1, i = 1, \cdots, N. \end{aligned} \tag{34}$$

For (34), the problem of view reconstruction based on phase optimization this then amounts to solving

$$\min_{\left|\hat{\phi}(\omega_t,\omega_v)\right|=1} Re\left(\hat{\phi}(\omega_t, \omega_v) \sum_{j\neq i} M_{i,j} \hat{\phi}^*(\omega_t, \omega_v)\right), \tag{35}$$

which means

$$\hat{\phi}(\omega_t, \omega_v) \approx \frac{1}{N} \sum_{i=1}^{N} \frac{-\sum_{j\neq i} M_{ij} arc\tan\left(\frac{P_I(\omega_t,\omega_v)}{P_R(\omega_t,\omega_v)}\right)}{\left|\sum_{j\neq i} M_{ij} arc\tan\left(\frac{P_I(\omega_t,\omega_v)}{P_R(\omega_t,\omega_v)}\right)\right|}, \tag{36}$$

for each $i = 1, \cdots, N$, when $\phi(\omega_t, \omega_v)$ is the optimum solution to problem (31).

REFERENCES

[1] S. J. Gortler, R. Grzeszczuk, R. Szeliski, and M. F. Cohen, "The lumigraph," in *Proc. 23rd Annu. Conf. Comput. Graph. Interact. Techn. (SIGGRAPH)*, 1996, pp. 43–54.
[2] M. Levoy and P. Hanrahan, "Light field rendering," in *Proc. 23rd Annu. Conf. Comput. Graph. Interact. Techn. (SIGGRAPH)*, 1996, pp. 31–40.
[3] M. Levoy, "Light fields and computational imaging," *Computer*, vol. 39, no. 8, pp. 46–55, Aug. 2006.

[4] J. Berent and P. L. Dragotti, "Plenoptic manifolds," *IEEE Signal Process. Mag.*, vol. 24, no. 6, pp. 34–44, Nov. 2007.

[5] C. Koniaris, M. Kosek, D. Sinclair, and K. Mitchell, "Compressed animated light fields with real-time view-dependent reconstruction," *IEEE Trans. Vis. Comput. Graphics*, vol. 25, no. 4, pp. 1666–1680, Apr. 2019.

[6] H. Jung, H.-J. Lee, and C. E. Rhee, "Flexibly connectable light field system for free view exploration," *IEEE Trans. Multimedia*, vol. 22, no. 4, pp. 980–991, Apr. 2020.

[7] C. Buehler, M. Bosse, L. Mcmillan, S. Gortler, and M. Cohen, "Unstructured lumigraph rendering," in *Proc. 28th Annu. Conf. Comput. Graph. Interact. Techn. (SIGGRAPH)*, 2001, pp. 425–432.

[8] G. Chaurasia, O. Sorkine, and G. Drettakis, "Silhouette-aware warping for image-based rendering," *Comput. Graph. Forum*, vol. 30, no. 4, pp. 1223–1232, 2011.

[9] C. Zhang and T. Chen, "Active rearranged capturing of image-based rendering scenes—Theory and practice," *IEEE Trans. Multimedia*, vol. 9, no. 3, pp. 520–531, Apr. 2007.

[10] F. Safaei, P. Mokhtarian, H. Shidanshidi, W. Li, M. Namazi-Rad, and A. Mousavinia, "Scene-adaptive configuration of two cameras using the correspondence field function," in *Proc. IEEE Int. Conf. Multimedia Expo. (ICME)*, Jul. 2013, pp. 1–6.

[11] C. Zhu, L. Yu, and Z. Xiong, "A noncoverage field model for improving the rendering quality of virtual views," *IEEE Trans. Multimedia*, vol. 20, no. 3, pp. 738–753, Mar. 2018.

[12] W. Zhou, A. Lumsdaine, and L. Lin, "Depth estimation with cascade occlusion culling filter for light-field cameras," in *Proc. 23rd Int. Conf. Pattern Recognit. (ICPR)*, Dec. 2016, pp. 1887–1892.

[13] T.-C. Wang, A. A. Efros, and R. Ramamoorthi, "Depth estimation with occlusion modeling using light-field cameras," *IEEE Trans. Pattern Anal. Mach. Intell.*, vol. 38, no. 11, pp. 2170–2181, Nov. 2016.

[14] C. Gilliam, P.-L. Dragotti, and M. Brookes, "On the spectrum of the plenoptic function," *IEEE Trans. Image Process.*, vol. 23, no. 2, pp. 502–516, Feb. 2014.

[15] C. J. Zhu and L. Yu, "Spectral analysis of image-based rendering data with scene geometry," *Multimedia Syst.*, vol. 23, no. 5, pp. 627–644, 2016.

[16] H. Hoshino, F. Okano, and I. Yuyama, "A study on resolution and aliasing for multi-viewpoint image acquisition," *IEEE Trans. Circuits Syst. Video Technol.*, vol. 10, no. 3, pp. 366–375, Apr. 2000.

[17] J. Stewart, J. Yu, S. J. Gortler, and L. McMillan, "A new reconstruction filter for undersampled light fields," in *Proc. Eurograph. Symp. Rendering (EGSR)*, Jun. 2003, pp. 150–156.

[18] G. Wu, Y. Liu, L. Fang, Q. Dai, and T. Chai, "Light field reconstruction using convolutional network on EPI and extended applications," *IEEE Trans. Pattern Anal. Mach. Intell.*, vol. 41, no. 7, pp. 1681–1694, Jul. 2019.

[19] G. Wu, B. Masia, A. Jarabo, Y. Zhang, L. Wang, Q. Dai, and Y. Liu, "Light field image processing: An overview," *IEEE J. Sel. Topics Signal Process.*, vol. 11, no. 7, pp. 926–954, Oct. 2017.

[20] R. Farrugia and C. Guillemot, "Light field super-resolution using a low-rank prior and deep convolutional neural networks," *IEEE Trans. Pattern Anal. Mach. Intell.*, vol. 42, no. 5, pp. 1162–1175, May 2020.

[21] N. Meng, H. K.-H. So, X. Sun, and E. Y. Lam, "High-dimensional dense residual convolutional neural network for light field reconstruction," *IEEE Trans. Pattern Anal. Mach. Intell.*, vol. 43, no. 3, pp. 873–886, Mar. 2021.

[22] Y. C. Eldar, N. Hammen, and D. G. Mixon, "Recent advances in phase retrieval," *IEEE signal Process. Mag.*, vol. 33, no. 5, pp. 158–162, Sep. 2016.

[23] Y. Schechtman, Y. C. Eldar, O. Cohen, H. N. Chapman, J. Miao, and M. Segev, "Phase retrieval with application to optical imaging: A contemporary overview," *IEEE Signal Process. Mag.*, vol. 32, no. 3, pp. 87–109, Mar. 2015.

[24] C. Zhu, H. Zhang, Y. Wei, N. He, and Q. Liu, "An iterative correction phase of light field for novel view reconstruction," in *Proc. MultiMedia Modeling (MMM)*. Cham, Switzerland: Springer, 2022, pp. 62–72.

[25] J. Jin, J. Hou, J. Chen, H. Zeng, S. Kwong, and J. Yu, "Deep coarse-to-fine dense light field reconstruction with flexible sampling and geometry-aware fusion," *IEEE Trans. Pattern Anal. Mach. Intell.*, vol. 44, no. 4, pp. 1819–1836, Apr. 2022, doi: 10.1109/TPAMI.2020.3026039.

[26] S. Vagharshakyan, R. Bregovic, and A. Gotchev, "Light field reconstruction using shearlet transform," *IEEE Trans. Pattern Anal. Mach. Intell.*, vol. 40, no. 1, pp. 133–147, Jan. 2018.

[27] Y. Gao, R. Bregovic, and A. Gotchev, "Self-supervised light field reconstruction using shearlet transform and cycle consistency," *IEEE Signal Process. Lett.*, vol. 27, pp. 1425–1429, 2020.

[28] L. Shi, H. Hassanieh, A. Davis, D. Katabi, and F. Durand, "Light field reconstruction using sparsity in the continuous Fourier domain," *ACM Trans. Graph.*, vol. 34, no. 1, p. 12, 2014.

[29] M. Le Pendu, C. Guillemot, and A. Smolic, "A Fourier disparity layer representation for light fields," *IEEE Trans. Image Process.*, vol. 28, no. 11, pp. 5740–5753, Nov. 2019.

[30] M. Zhou, Y. Ding, Y. Ji, S. S. Young, J. Yu, and J. Ye, "Shape and reflectance reconstruction using concentric multi-spectral light field," *IEEE Trans. Pattern Anal. Mach. Intell.*, vol. 42, no. 7, pp. 1594–1605, Jul. 2020.

[31] M. Marquez, H. Rueda-Chacon, and H. Arguello, "Compressive spectral light field image reconstruction via online tensor representation," *IEEE Trans. Image Process.*, vol. 29, pp. 3558–3568, 2020.

[32] G. Wu, M. Zhao, L. Wang, Q. Dai, T. Chai, and Y. Liu, "Light field reconstruction using deep convolutional network on EPI," in *Proc. IEEE Conf. Comput. Vis. Pattern Recognit. (CVPR)*, Jul. 2017, pp. 1638–1646.

[33] G. Wu, Y. Liu, L. Fang, and T. Chai, "Revisiting light field rendering with deep anti-aliasing neural network," *IEEE Trans. Pattern Anal. Mach. Intell.*, early access, Apr. 16, 2021, doi: 10.1109/TPAMI.2021.3073739.

[34] G. Wu, Y. Liu, Q. Dai, and T. Chai, "Learning sheared EPI structure for light field reconstruction," *IEEE Trans. Image Process.*, vol. 28, no. 7, pp. 3261–3273, Jul. 2019.

[35] M. Lamba, K. K. Rachavarapu, and K. Mitra, "Harnessing multi-view perspective of light fields for low-light imaging," *IEEE Trans. Image Process.*, vol. 30, pp. 1501–1513, 2021.

[36] Z. Hu, H. W. F. Yeung, X. Chen, Y. Y. Chung, and H. Li, "Efficient light field reconstruction via spatio-angular dense network," *IEEE Trans. Instrum. Meas.*, vol. 70, pp. 1–14, 2021.

[37] D. Liu, Y. Huang, Q. Wu, R. Ma, and P. An, "Multi-angular epipolar geometry based light field angular reconstruction network," *IEEE Trans. Comput. Imag.*, vol. 6, pp. 1507–1522, 2020.

[38] A. K. Vadathya, S. Girish, and K. Mitra, "A unified learning-based framework for light field reconstruction from coded projections," *IEEE Trans. Comput. Imag.*, vol. 6, pp. 304–316, 2020.

[39] Y. Wang, F. Liu, K. Zhang, Z. Wang, Z. Sun, and T. Tan, "High-fidelity view synthesis for light field imaging with extended pseudo 4DCNN," *IEEE Trans. Comput. Imag.*, vol. 6, pp. 830–842, 2020.

[40] J. Jin, J. Hou, J. Chen, H. Zeng, S. Kwong, and J. Yu, "Deep coarse-to-fine dense light field reconstruction with flexible sampling and geometry-aware fusion," *IEEE Trans. Pattern Anal. Mach. Intell.*, vol. 44, no. 4, pp. 1819–1836, Apr. 2022.

[41] P. Chandramouli, K. V. Gandikota, A. Goerlitz, A. Kolb, and M. Moeller, "A generative model for generic light field reconstruction," *IEEE Trans. Pattern Anal. Mach. Intell.*, vol. 44, no. 4, pp. 1712–1724, Apr. 2022.

[42] M. Hayes, J. Lim, and A. Oppenheim, "Signal reconstruction from phase or magnitude," *IEEE Trans. Acoust., Speech, Signal Process.*, vol. ASSP-28, no. 6, pp. 672–680, Dec. 1980.

[43] K. Jaganathan, S. Oymak, and B. Hassibi, "Sparse phase retrieval: Uniqueness guarantees and recovery algorithms," *IEEE Trans. Signal Process.*, vol. 65, no. 9, pp. 2402–2410, May 2017.

[44] Q. Li, L. Huang, W. Liu, B. Zhao, and P. Zhang, "Carrier phase recovery for array navigation receiver: A fast phase retrieval approach," *IEEE Access*, vol. 7, pp. 179385–179395, 2019.

[45] Y. Geng, X. Wen, J. Tan, S. Liu, and Z. Liu, "Noise-robust phase retrieval by optics path modulation with adaptive feedback," *Opt. Commun.*, vol. 515, pp. 128–199, Jul. 2022.

[46] Z. Liu, H. Chen, W. Blondel, J. Tan, Z. Song, Z. Hu, C. Tan, and S. Liu, "Generation of hollow beams by using phase filtering with multi-distance phase retrieval," *Opt. Commun.*, vol. 456, Feb. 2020, Art. no. 124611.

[47] L. Taylor, "The phase retrieval problem," *IEEE Trans. Antennas Propag.*, vol. AP-29, no. 2, pp. 386–391, Mar. 1981.

[48] J. R. Fienup, "Phase retrieval algorithms: A comparison," *Appl. Opt.*, vol. 21, no. 15, pp. 2758–2769, Aug. 1982.

[49] M. V. Klibanov, P. E. Sacks, and A. V. Tikhonravov, "The phase retrieval problem," *Inverse Problems*, vol. 11, no. 1, pp. 1–28, 1995.

[50] I. Waldspurger, A. D'Aspremont, and S. Mallat, "Phase recovery, MaxCut and complex semidefinite programming," *Math. Programm.*, vol. 149, nos. 1–2, pp. 47–81, 2015.

[51] E. J. Candes, Y. C. Eldar, T. Strohmer, and V. Voroninski, "Phase retrieval via matrix completion," *SIAM Rev.*, vol. 57, no. 2, pp. 225–251, 2015.

[52] E. J. Candès, X. Li, and M. Soltanolkotabi, "Phase retrieval via Wirtinger flow: Theory and algorithms," *IEEE Trans. Inf. Theory*, vol. 61, no. 4, pp. 1985–2007, Apr. 2015.

[53] J. Sun, Q. Qu, and J. Wright, "A geometric analysis of phase retrieval," *Found. Comput. Math.*, vol. 18, pp. 1131–1198, pp. 1–68, Oct. 2018.
[54] J.-X. Chai, S.-C. Chan, H.-Y. Shum, and X. Tong, "Plenoptic sampling," in *Proc. 27th Annu. Conf. Comput. Graph. Interact. Techn. (SIGGRAPH)*, 2000, pp. 307–318.
[55] C. Zhang and T. Chen, "Spectral analysis for sampling image-based rendering data," *IEEE Trans. Circuits Syst. Video Technol.*, vol. 13, no. 11, pp. 1038–1050, Nov. 2003.
[56] M. N. Do, D. Marchand-Maillet, and M. Vetterli, "On the bandwidth of the plenoptic function," *IEEE Trans. Image Process.*, vol. 21, no. 2, pp. 708–717, Feb. 2012.
[57] C. Zhu, L. Yu, Z. Yan, and S. Xiang, "Frequency estimation of the plenoptic function using the autocorrelation theorem," *IEEE Trans. Comput. Imag.*, vol. 3, no. 4, pp. 966–981, Dec. 2017.
[58] R. C. Bolles, H. H. Baker, and D. H. Marimont, "Epipolar-plane image analysis: An approach to determining structure from motion," *Int. J. Comput. Vis.*, vol. 1, no. 1, pp. 7–55, 1987.
[59] Accessed: Feb. 7, 2022. [Online]. Available: http://lightfield.stanford.edu/

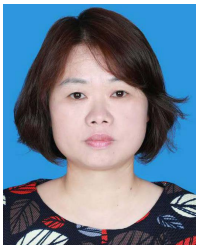

NAN HE received the B.M. and M.S. degrees in computer and its application from South Central University for Nationalities, Wuhan, China, in 1996 and 2004, respectively. She is currently an Associate Professor with the Department of Mathematics and Computer Science, Guilin Normal College, Guilin, China. Her research interests include graphics and image processing.

HONG ZHANG received the B.S. degree in education of physics from Huazhong Normal University, Wuhan, China, in 2006, and the M.S. degree in computer software and theory from Guangxi Normal University, Guilin, China, 2009. She is currently a Lecturer with the Department of Mathematics and Computer Science, Guilin Normal College, Guilin. Her research interests include multimedia signal processing and multimedia communication.

CHANGJIAN ZHU (Member, IEEE) received the B.S. degree in electronics and information engineering and the M.S. degree in electronic circuit and system from Guangxi Normal University, Guilin, China, in 2006 and 2009, respectively, and the Ph.D. degree from the School of Electronic Information and Communications, Huazhong University of Science and Technology, Wuhan, China, in 2017. He is currently an Associate Professor with Guangxi Normal University. He is also a Senior Researcher with the College of Electronics and Information Engineering, Shenzhen University. His research interests include light field sampling and applications of sampling theory to image processing in particular image-based rendering.